Fundamental limits on the rate of bacterial cell division

Nathan M. Belliveau[†, 1], **Griffin Chure**[†, 2, 3], **Christina L. Hueschen**[4], **Hernan G. Garcia**[5], **Jane Kondev**[6], **Daniel S. Fisher**[7], **Julie A. Theriot**[1, 8], **Rob Phillips**[2, 9, *]

***For correspondence:**

[†]These authors contributed equally to this work

[1]Department of Biology, University of Washington, Seattle, WA, USA; [2]Division of Biology and Biological Engineering, California Institute of Technology, Pasadena, CA, USA; [3]Department of Applied Physics, California Institute of Technology, Pasadena, CA, USA; [4]Department of Chemical Engineering, Stanford University, Stanford, CA, USA; [5]Department of Molecular Cell Biology and Department of Physics, University of California Berkeley, Berkeley, CA, USA; [6]Department of Physics, Brandeis University, Waltham, MA, USA; [7]Department of Applied Physics, Stanford University, Stanford, CA, USA; [8]Allen Institute for Cell Science, Seattle, WA, USA; [9]Department of Physics, California Institute of Technology, Pasadena, CA, USA; [*]Contributed equally

Abstract This will be written next (promise).

Synthesis of the Cell Envelope

The subjects of our estimates thus far have been localized to the periphery of the cell, embedded within the hydrophobic lipid bilayer of the inner membrane. As outlined in **??**, cells could in principle increase the expression of the membrane-bound ATP synthases and electron transport chains to support a larger energy budget across a wide range of cell volumes and membrane surface areas. This ability, however, is contingent on the ability of the cell to expand the surface area of the cell by synthesizing new lipids and peptidoglycan for the cell wall. In this next class of estimates, we will turn our focus to these processes and consider the copy numbers of the relevant enzymes.

Lipid Synthesis

The cell envelopes of gram negative bacteria (such as *E. coli*) are composed of inner and outer phospholipid bilayer membranes separated by a ≈ 10 nm periplasmic space (BNID: 100016, ***Milo et al.*** (***2010***)). As mentioned in our discussion of the surface area to volume constraints on energy production, *E. coli* is a rod-shaped bacterium with a 4:1 length-to-width aspect ratio. At modest growth rates, such as our stopwatch of 5000 s, the total cell surface area is ≈ 5 μm^2 (BNID: 101792, ***Milo et al.*** (***2010***)). As there are two membranes, each of which composed of two lipid leaflets, the total membrane area is ≈ 20μm^2, a remarkable value compared to the ≈ 2μm length of the cell.

While this represents the total area of the membrane, this does not mean that it is composed entirely of lipid molecules. Rather, the dense packing of the membrane with proteins means that only ≈ 40 % of the membrane area is occupied by lipids (BNID: 100078, ***Milo et al.*** (***2010***)). Using a rule-of-thumb of 0.5 nm^2 as the surface area of the typical lipid (BNID: 106993, ***Milo et al.*** (***2010***)), we arrive at an estimate of $\approx 2 \times 10^7$ lipids per cell, an estimate in close agreement with experimental measurements (BNID: 100071, 102996; ***Milo et al.*** (***2010***)).

The membranes of *E. coli* are composed of a variety of different lipids, each of which are unique in their structures and biosynthetic pathways (***Sohlenkamp and Geiger, 2016***). With such diversity

in biosynthesis, it becomes difficult to identify which step(s) may be the rate-limiting, an objective further complicated by the sparsity of *in vivo* kinetic data. Recently, a combination of stochastic kinetic modeling (***Ruppe and Fox, 2018***) and *in vitro* kinetic measurements (***Ranganathan et al., 2012***; ***Yu et al., 2011***) have revealed remarkably slow steps in the fatty acid synthesis pathways which may serve as the rate limiting reactions. One such step is the removal of hydroxyl groups from the fatty-acid chain by ACP dehydratase that leads to the formation of carbon-carbon double bonds. This reaction, catalyzed by proteins FabZ and FabA in *E. coli* (***Yu et al., 2011***), have been estimated to have kinetic turnover rates of ≈ 1 dehydration per second per enzyme (***Ruppe and Fox, 2018***). Combined with this rate, our previous estimates for the number of lipids to be formed, and a 5000 second division yields an estimate that the cell requires ≈ 4000 ACP dehydratases. This is in reasonable agreement with the experimentally observed copy numbers of FabZ and FabA (***Figure 1***(A)). Furthermore, we can extend this estimate to account for the change in membrane surface area as a function of the growth rate (grey line in ***Figure 1***(A)), which captures the observed growth rate dependent expression of these two enzymes.

Despite the slow catalytic rate of FabZ and FabA, we argue that the generation of fatty acids is not a bottleneck in cell division and is not the key process responsible for setting the bacterial growth rate. Experimental evidence has shown that the rate of fatty-acid synthesis can be drastically increased *in vitro* by increasing the concentration of FabZ ***Yu et al.*** (***2011***). Stochastic simulations of the complete fatty acid synthesis pathway of *E. coli* further supports this experimental observation ***Ruppe and Fox*** (***2018***). Thus, if this step was the determining factor in cell division, increasing growth rate could be as simple as increasing the number of ACP dehydratases per cell. With a proteome size of $\approx 3\times10^6$ proteins, a hypothetical increase in expression from 4000 to 40,000 ACP dehydratases would result in a $\approx 1\%$ increase in the size of the proteome. As many other proteins are in much larger abundance than 4000 per cell (as we will see in the coming sections), it is unlikely that expression of ACP dehydratases couldn't be increased to facilitate faster growth.

Peptidoglycan Synthesis

While variation in cell size can vary substantially across growth conditions, bacterial cells demonstrate exquisite control over their cell shape. This is primarily due to the cell wall, a stiff meshwork of polymerized discaccharides interspersed with short peptide crosslinks termed the peptidoglycan. The cell wall is also a vital structural component that counteracts turgor pressure. In *E. coli*, this enormous peptidoglycan molecule is a few nanometers thick and resides within the periplasmic space between the inner and outer membrane. The formation of the peptidoglycan is an intricate process, involving the bacterial actin homolog MreB (***Shi et al., 2018***) along with a variety of membrane-bound and periplasmic enzymes (***Morgenstein et al., 2015***). The coordinated action of these components result in a highly-robust polymerized meshwork that maintains cell shape even in the face of large-scale perturbations and can restore rod-shaped morphology even after digestion of the peptidoglycan (***Harris and Theriot, 2018***; ***Shi et al., 2018***).

In glucose-supported steady-state growth, the peptidoglycan alone comprises $\approx 3\%$ of the cellular dry mass (BNID: 101936, ***Milo et al.*** (***2010***)), making it the most massive molecule in *E. coli*. The polymerized unit of the peptidoglycan is a N-acetylglucosamine and N-acetylmuramic acid disaccharide, of which the former is functionalized with a short pentapeptide. With a mass of ≈ 1000 Da, this unit, which we refer to as a murein monomer, is polymerized to form long strands in the periplasm which are then attached to each other via their peptide linkers. Using the aforementioned measurement that $\approx 3\%$ of the dry mass is peptidoglycan, it can be estimated that the peptidoglycan is composed of $\approx 6\times10^6$ murein monomers.

During growth, peptidoglycan is constantly being broken down to allow insertion of new murein monomers and cellular expansion. In order to maintain structural integrity these monomers must be crosslinked into the expanding cell wall, potentially limiting how quickly new material can be added and we consider this process as a possible rate-limiting step. In principle, each one of these murein monomers can be crosslinked to another glycan strand via the pentapeptide. In

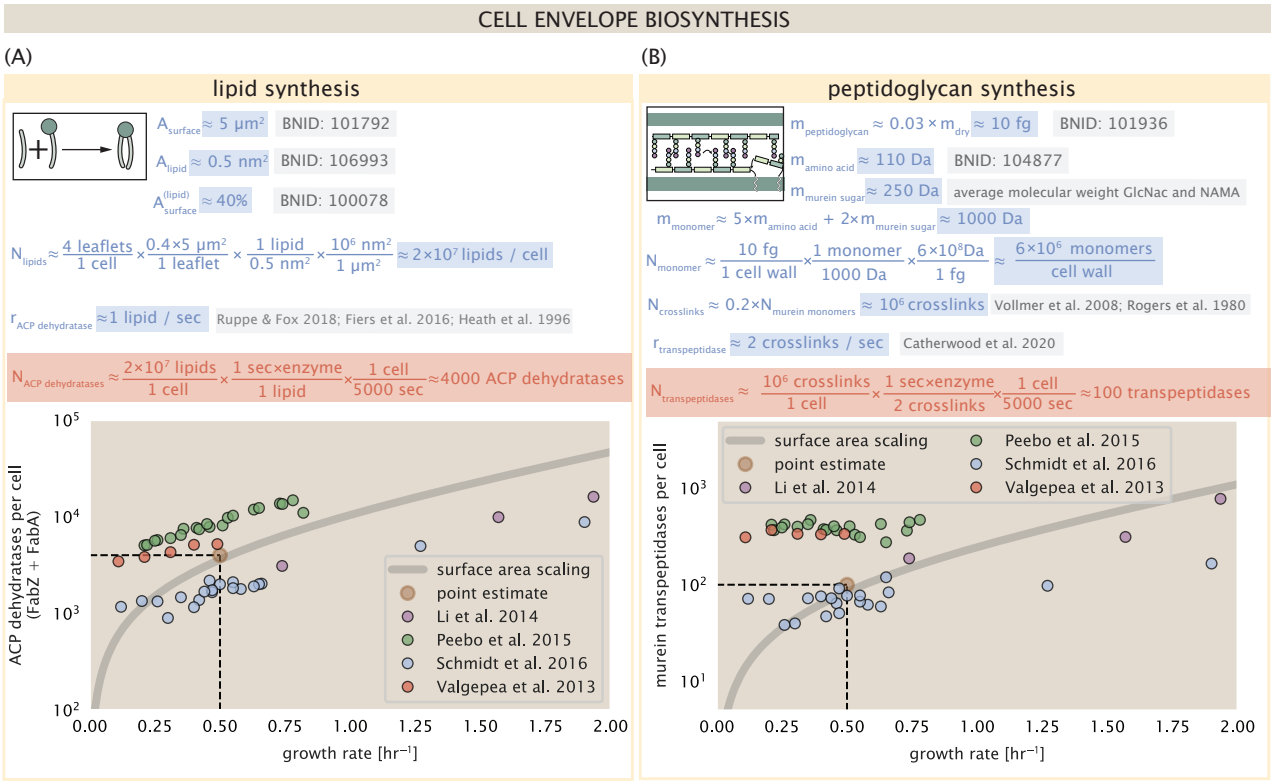

Figure 1. Estimation of the key components involved in cell envelope biosynthesis. (A) Top panel shows an estimation for the number of ACP dehydratases necessary to form functional phospholipids, which is assumed to be a rate-limiting step on lipid synthesis. The rate of ACP dehydratases was inferred from experimental measurements via a stochastic kinetic model described in ***Ruppe and Fox*** (***2018***). Bottom panel shows the experimentally observed complex copy numbers using the stoichiometries $[FabA]_2$ and $[FabZ]_2$. (B) An estimate for the number of peptidoglycan transpeptidases needed to complete maturation of the peptidoglycan. The mass of the murein monomer was estimated by approximating each amino acid in the pentapeptide chain as having a mass of 110 Da and each sugar in the disaccharide having a mass of ≈ 250 Da. The *in vivo* rate of transpeptidation rein *E. coli* was taken from recent analysis by ***Catherwood et al.*** (***2020***). The bottom panel shows experimental measurements of the transpeptidase complexes in *E. coli* following the stoichiometries $[MrcA]_2$, $[MrcB]_2$, $[MrdA]_1$, and $[MrdB]_1$. Grey curves in each plot show the estimated number of complexes needed to satisfy the synthesis requirements scaled by the surface area as a function of growth rate. We direct the reader to the supplemental information for a more detailed discussion of this estimate.

some species, such as in gram-positive bacterium *Staphylococcus aureus*, the extent of crosslinking can be large with > 90% of pentapeptides forming a connection between glycan strands. In *E. coli*, however, a much smaller proportion (≈ 20%) of the peptides are crosslinked, resulting in a weaker and more porous cell wall ***Vollmer et al.*** (***2008***); ***Rogers et al.*** (***1980***). The formation of these crosslinks primarily occur during the polymerization of the murein monomers and is facilitated by a family of enzymes called transpeptidases. In *E. coli*, there are four primary transpeptidases that are involved in lateral and longitudinal extension of the peptidoglycan. These transpeptidases have only recently been quantitatively characterized *in vivo* via liquid chromatography mass spectrometry (***Catherwood et al., 2020***), which revealed a kinetic turnover rate of $\approx 1-2$ crosslinking reactions formed per second per enzyme.

Pulling these measurements together permits us to make an estimate that on the order of ≈ 100 transpeptidases are needed for complete maturation of the peptidoglycan, given a division time of ≈ 5000 seconds, a value that is closely aligned with the experimental observations (***Figure 1***(B)). Expanding this estimate to account for the changing volume of the peptidoglycan as a function of growth rates (grey line in ***Figure 1***(B)) also qualitatively captures the observed dependence in the data, though systematic disagreements between the different data sets makes the comparison more difficult.

Much as in the case of fatty acid synthesis, we find it unlikely that the formation of peptidoglycan is a rate limiting step in bacterial cell division. The estimate we have presented considered only the transpeptidase enzymes that are involved lateral and longitudinal elongation of the peptidoglycan (proteins MrdA, MrdB, MrcA, and MrcB). This neglects the presence of other transpeptidases that are present in the periplasm and also involved in remodeling and maturation of the peptidoglycan. It is therefore possible that if this was setting the speed limit for cell division, the simple expression of more transpeptidases may be sufficient to maintain the structural integrity of the cell wall.

While this dependence between cell size and ribosomal abundance is apparent across moderate to fast growth rates, it is worth noting that this scaling is likely to change at slow growth rates (below $\lambda \approx 0.5\,\mathrm{hr}^{-1}$). Here, the number of ribosomes R no longer reflects the cell's protein synthesis capacity, so far taken to be $r_t \times R$. Instead, cells reduce the number of actively translating ribosomes through the additional regulatory control of the small-molecule alarmone, guanosine pentaphosphate [(p)ppGpp] (***Dai et al., 2016***) [more citations].

E. coli Maximizes Steady-State Growth Rate by Tuning both Ribosomal Content and Translation Activity.

The translation-limited growth rate (**??**) highlights the necessity for a cell to increase its ribosomal fraction to maximize its growth rate. However, it ignores the absolute constraints of a growing cell, which in particular, require resources to support each translating ribosomes and the space to house them. For almost every one of our estimates, the proteomic data suggest that cells predominantly vary their protein abundances in order to keep pace with the demands of a growing cell. In this final section we consider a minimal model of growth rate control. We use it to provide intution into the additional constraints that arise when growth rate and ribosomal abudance is intimately tied to cell size.

[do I talk about ppGpp and nutrient sensing? Maybe later once I show the trends]

In order for cells to maxmize their rate of protein synthesis, $r_t \times R$, ribosomes must be able to rapidly match codons with their correct amino-acyl tRNAs. This requires synthesis of (or import, for rich media) amino acids that maintain the pool of amino-acyl tRNAs. To proceed, we therefore consider this maintenance as simply a balance between the the supply of amino acids by metabolic proteins and transporters, at a rate of r_{aa} in units of amino acids per second, and consumption by ribosomes at a rate of $r_t \times R \times f_a$. The addition factor f_a is the fraction of actively translating ribosomes, and allows us to account for the possibility of nonfunctional, immature ribosomes or active sequentration of ribosomes mediated by (p)ppGpp at slow growth (***Dennis et al., 2004***; ***Dai et al., 2016***). During steady-state growth, we can assume that amino acid concentration, denoted

by an effective pool $[AA]_{\text{eff}}$, is constant ($d[AA]_{\text{eff}}/dt$=0). The rates of suppy and consumption are related to $[AA]_{\text{eff}}$ over an average cell cycle by,

$$\int_0^\tau \frac{d[AA]_{\text{eff}}}{dt} dt = \frac{1}{V} \int_0^\tau (r_a a - r_t \; R \; f_a) dt, \tag{1}$$

[important point is that as resources become limiting, cells are able to tune and minimize the entire cell mass - which enables them to grow faster]

[Discuss implications of findings so far. All other components being tuned (mostly) in the required proportions; and also that the achievable growth rate is ultimately set by ribosomes.]

[The apparent constraint that cells MUST get larger in order to grow faster places a particular constrain on why a cell would vary its ribosomal fraction in the first place.]

[Also present the evidence from literature that there is a prominent role for aa/nutrient sensing that appears to mediate X, Y, and Z.]

[Then go on to propose the way to understand what's going on with our model. - I think maybe it's easiest to understand it is we start by considering the balance that must be maintained between metabolic activity and ribosomal activity. - Then write down a model that relates how elongation rate will relate to this.]

gives no intuition into the additional constraints of a growing cell that we've consider throughout our estimates.

quantifies the maximum rate of growth but ignores the additional constraint set that there is a maximum rate us with a maximum

[Figure idea: PART (A) Maybe we can consider that $r_t * R sets the maximum rate of growth; but you also need to feed t$

[When I get into slow growth regime; consider that IF R scales with <ori>, ribosomes will have increasingly longer wait times for protein synthesis. Which is bad. - By also decreasing the fraction of actively translating ribosomes, cells can grow faster is also super important.]

As a final comment, it has recently been shown that growth in a (p)ppGpp null strain also lacked both the condition-dependent changes in ⟨# ori⟩ as well as changes in cell size across different growth condition. Instead, cells always exhibited a high ratio of ⟨# ori⟩ to ⟨# ter⟩, irrespective of growth rate, and a cell size that was more consistent with a fast growth state where (p)ppGpp levels are normally low (***Fernández-Coll et al., 2020***) and ribosomal fraction is high (***Zhu and Dai, 2019***). There is also evidence that this may be achived through inhibition of DNA replication initiation (***Kraemer et al., 2019***). These observations raise the possibility that (p)ppGpp may be playing a causal role in tuning ⟨# ori⟩ and cell size, which ultimately allows the cell to vary its ribosomal content according to nutrient availability.

References

Catherwood AC, Lloyd AJ, Tod JA, Chauhan S, Slade SE, Walkowiak GP, Galley NF, Punekar AS, Smart K, Rea D, Evans ND, Chappell MJ, Roper DI, Dowson CG. Substrate and Stereochemical Control of Peptidoglycan Cross-Linking by Transpeptidation by Escherichia Coli PBP1B. Journal of the American Chemical Society. 2020 Mar; 142(11):5034–5048. doi: 10.1021/jacs.9b08822.

Dai X, Zhu M, Warren M, Balakrishnan R, Patsalo V, Okano H, Williamson JR, Fredrick K, Wang YP, Hwa T. Reduction of translating ribosomes enables *Escherichia coli* to maintain elongation rates during slow growth. Nature Microbiology. 2016 Dec; 2(2):16231.

Dennis PP, Ehrenberg M, Bremer H. Control of rRNA Synthesis in Escherichia coli: a Systems Biology Approach. Microbiology and Molecular Biology Reviews. 2004 Dec; 68(4):639–668.

Fernández-Coll L, Maciag-Dorszynska M, Tailor K, Vadia S, Levin PA, Szalewska-Palasz A, Cashel M, Dunny GM. The Absence of (p)ppGpp Renders Initiation of *Escherichia coli* Chromosomal DNA Synthesis Independent of Growth Rates. mBio. 2020 Apr; 11(2):45.

Harris LK, Theriot JA. Surface Area to Volume Ratio: A Natural Variable for Bacterial Morphogenesis. Trends in microbiology. 2018 Oct; 26(10):815–832.

Kraemer JA, Sanderlin AG, Laub MT. The Stringent Response Inhibits DNA Replication Initiation in E. coliby Modulating Supercoiling of oriC. mBio. 2019 Aug; 10(4):822.

Milo R, Jorgensen P, Moran U, Weber G, Springer M. BioNumbers—the Database of Key Numbers in Molecular and Cell Biology. Nucleic Acids Research. 2010 Jan; 38(suppl_1):D750–D753. doi: 10.1093/nar/gkp889.

Morgenstein RM, Bratton BP, Nguyen JP, Ouzounov N, Shaevitz JW, Gitai Z. RodZ Links MreB to Cell Wall Synthesis to Mediate MreB Rotation and Robust Morphogenesis. Proceedings of the National Academy of Sciences. 2015 Oct; 112(40):12510–12515. doi: 10.1073/pnas.1509610112.

Ranganathan S, Tee TW, Chowdhury A, Zomorrodi AR, Yoon JM, Fu Y, Shanks JV, Maranas CD. An Integrated Computational and Experimental Study for Overproducing Fatty Acids in Escherichia Coli. Metabolic Engineering. 2012 Nov; 14(6):687–704. doi: 10.1016/j.ymben.2012.08.008.

Rogers H, Perkins H, Ward J. Microbial Cell Walls and Membranes. London: Chapman and Halll; 1980.

Ruppe A, Fox JM. Analysis of Interdependent Kinetic Controls of Fatty Acid Synthases. ACS Catalysis. 2018 Dec; 8(12):11722–11734. doi: 10.1021/acscatal.8b03171.

Shi H, Bratton BP, Gitai Z, Huang KC. How to Build a Bacterial Cell: MreB as the Foreman of E. Coli Construction. Cell. 2018 Mar; 172(6):1294–1305. doi: 10.1016/j.cell.2018.02.050.

Sohlenkamp C, Geiger O. Bacterial Membrane Lipids: Diversity in Structures and Pathways. FEMS Microbiology Reviews. 2016 Jan; 40(1):133–159. doi: 10.1093/femsre/fuv008.

Vollmer W, Blanot D, De Pedro MA. Peptidoglycan Structure and Architecture. FEMS Microbiology Reviews. 2008 Mar; 32(2):149–167. doi: 10.1111/j.1574-6976.2007.00094.x.

Yu X, Liu T, Zhu F, Khosla C. In Vitro Reconstitution and Steady-State Analysis of the Fatty Acid Synthase from Escherichia Coli. Proceedings of the National Academy of Sciences. 2011 Nov; 108(46):18643–18648. doi: 10.1073/pnas.1110852108.

Zhu M, Dai X. Growth suppression by altered (p)ppGpp levels results from non-optimal resource allocation in *Escherichia coli*. Nucleic Acids Research. 2019 Mar; 47(9):4684–4693.